THE EFFECT OF A CHANGE IN ORIENTATION OF A RECTANGULAR FOUR-PADDLE SOLAR ARRAY ON THE SPIN RATE OF A SATELLITE

by

S. G. McCarron

January 1966

Goddard Space Flight Center
Greenbelt, Maryland

THE EFFECT OF A CHANGE IN ORIENTATION
OF A RECTANGULAR FOUR-PADDLE SOLAR ARRAY
ON THE SPIN RATE OF A SATELLITE

S. G. McCarron

SUMMARY 19484

Two cases of spin-rate dependence of a four-paddle satellite are analyzed: (1) the case where the spin rate changes by varying the paddle-spar angle, holding the paddle-pitch angle constant, and (2) the case where the spin rate changes by varying the paddle-pitch angle, holding the paddle-spar angle constant. In both cases it is assumed that component mass homogeneity exists, the same variation in paddle-pitch or paddle-spar angles occurs simultaneously on all four solar paddles, and external torques (aerodynamic, solar radiation, etc.) are negligible over a short period of time. Conditions are discussed for satellite normalized-spin-rate decay or growth based solely on solar-array geometry.

In the appendices are curves of the solar-paddle moment of inertia, paddle-arm moment of inertia, and satellite normalized-spin rates, as a function of orientation for the laboratory model satellite, as well as, for a full scale IMP-type satellite.

auth

CONTENTS

SYMBOLS

a	rectangular-solar-paddle width
b	rectangular-solar-paddle length
c	rectangular-solar-paddle thickness (mean thickness in the case of a symmetrical-tapered paddle)
$H(p)$	satellite angular momentum as a function of paddle-pitch angle
$H_0(p)$	$H(p)$ evaluated at the paddle-pitch angle zero
$H(\theta)$	satellite angular momentum as a function of paddle-spar angle
$H_0(\theta)$	$H(\theta)$ evaluated at the paddle-spar angle zero
h	satellite-body height
$I_{A_{zz}}(\theta)$	paddle-arm moment of inertia about the z-axis of the nonspinning configurational coordinate system
$I_{A_{zz}}(0)$	$I_{A_{zz}}$ evaluated at the paddle-spar angle zero
$I_{B_{zz}}$	satellite-body moment of inertia about its spin axis
$I_{P_{zz}}(p,\theta)$	solar-paddle moment of inertia about the z-axis of the nonspinning configurational coordinate system
$I_{P_{zz}}(0,\theta)$	$I_{P_{zz}}$ evaluated at the paddle-pitch angle zero
$I_{P_{zz}}(p,0)$	$I_{P_{zz}}$ evaluated at the paddle-spar angle zero
M_A	paddle-arm mass
M_B	satellite-body mass
M_P	solar-paddle mass
p	paddle-pitch angle (the acute angle the plane of the paddle makes with the θ unit vector)

R   octagon-face radius (circumscribed radius)

r   octagon-face apothem (inscribed radius)

r_A paddle-arm cross-section radius

s   octagon-base edge

v   volume

x y z   nonspinning configurational coordinate system of the satellite

$\left.\begin{array}{l} x_1 \, y_1 \, z_1 \\ x_2 \, y_2 \, z_2 \\ x_3 \, y_3 \, z_3 \\ x_4 \, y_4 \, z_4 \end{array}\right\}$ rotated, translated, or rotated-translated coordinate systems with respect to the nonspinning configurational coordinate system of the satellite

α octagon-prism-sector angle

θ paddle-spar angle (the angle the paddle spar subtends with the negative z-axis of the configurational coordinate system)

λ cylindrical-paddle-arm length

ρ_v mean density

ω_{z_p} satellite angular velocity dependent on paddle-pitch angle (paddle-spar angle constant)

$\omega_{z_{p_0}}$ ω_{z_p} evaluated at the paddle-pitch angle zero

ω_{z_θ} satellite angular velocity dependent on paddle-spar angle (paddle-pitch angle constant)

$\omega_{z_{\theta_0}}$ ω_{z_θ} evaluated at the paddle-spar angle zero

THE EFFECT OF A CHANGE IN ORIENTATION
OF A RECTANGULAR FOUR-PADDLE SOLAR ARRAY
ON THE SPIN RATE OF A SATELLITE

INTRODUCTION

Solar-paddle-orientation studies were initiated in order to improve the specific power (power per unit weight) of a solar-paddle array. The beneficial results derived from an active orientation system are: (1) the lessening of shadowing effects (paddle-on-paddle and/or body-on-paddle shading of the solar cells composing the array), (2) the decreasing of array-aspect variation, and/or (3) the changing of sun aspect to compensate as the ill effects of radiation damage and micrometeorite bombardment take their toll during the lifetime of the array. It was with these thoughts in mind that a model satellite was constructed with a configuration along the lines of an IMP-type satellite. Since these arrays are for spin-stabilized satellites, any change in the array orientation will change the moment of inertia of the satellite and hence the satellite spin rate. Figure 1 shows the satellite configuration with two orientation angles defined so as to simplify the analysis in the development of generalized expressions.

MOMENT OF INERTIA ANALYSIS

Octagonal Satellite Body

The octagonal body of the satellite is shown in Figure 2. In the analysis it is assumed that mass homogeneity exists for the body and that the spin axis is the z-axis of figure symmetry. Let s be the length of an edge, h be the height, R be the circumscribed radius, α be the segment angle, and r be the apothem of an octagonal face. Then the moment of inertia about the spin axis of the prism is given by

$$I_{B_{zz}} = \int_m (x^2 + y^2)\, dm = 16\, \rho_v \int_{-h/2}^{h/2} \int_0^r \int_0^{y\, \tan\frac{\alpha}{2}} (x^2 + y^2)\, dx\, dy\, dz \qquad (1)$$
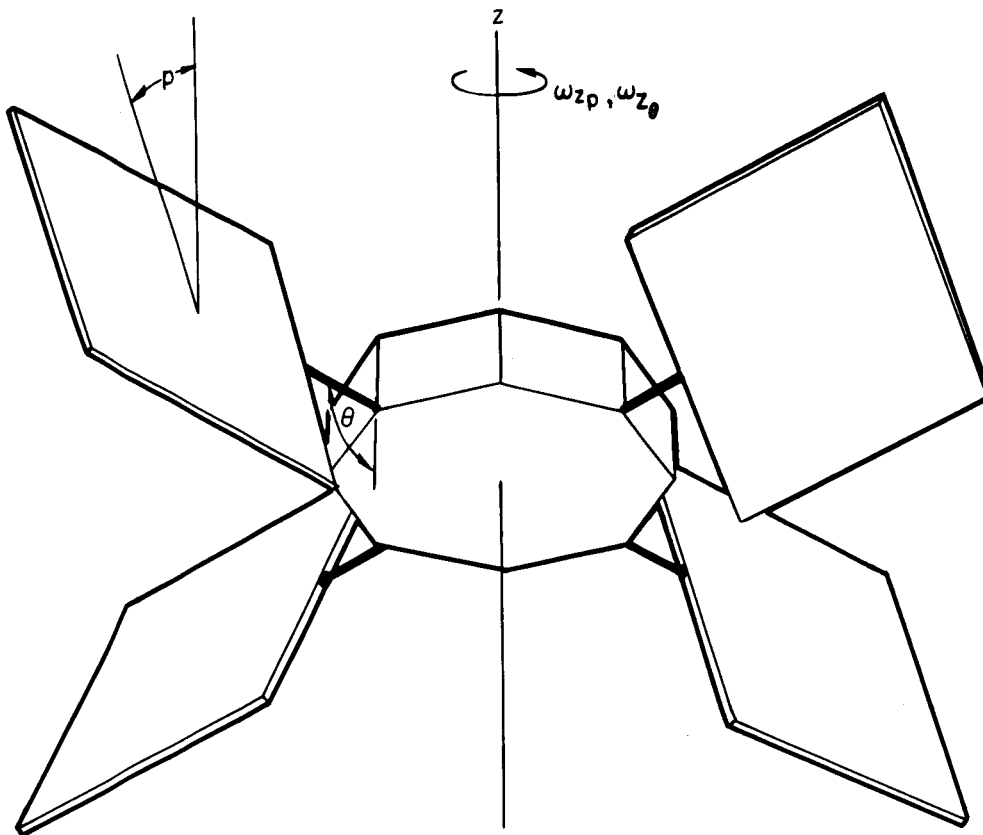
1

Figure 1–IMP-type satellite depicting the variable four-paddle solar array
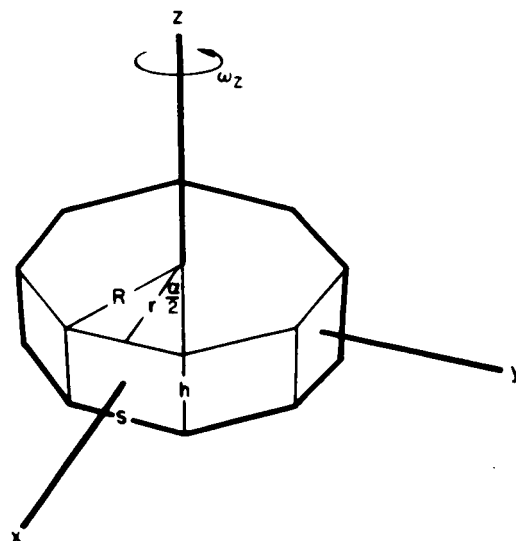with two orientation angles.

Figure 2–IMP-type satellite body in the nonspinning
configurational coordinate system.

2

where ρ_v is the uniform mass density of the body. Integration of Eq. (1) gives

$$I_{B_{zz}} = \frac{M_B}{24}(s^2 + 12\ r^2) \tag{2}$$

where M_B is the mass of the satellite body.

Cylindrical Paddle Arm

One of the cylindrical paddle arms is shown in Figure 3. The arm is assumed to be of homogeneous mass and the $x_4 y_4 z_4$ triad to be the axes of figure symmetry. The length of the arm is designated by λ and the cross sectional radius is labeled r_A. The $x_1 y_1 z_1$ triad as shown in Figure 4 is related to the $x_4 y_4 z_4$ triad by the transformation matrix

$$\begin{pmatrix} x_1 \\ y_1 \\ z_1 \end{pmatrix} = \begin{pmatrix} \sin\theta & 0 & \cos\theta \\ 0 & 1 & 0 \\ -\cos\theta & 0 & \sin\theta \end{pmatrix} \begin{pmatrix} x_4 \\ y_4 \\ z_4 \end{pmatrix} \tag{3}$$

The xyz nonspinning coordinate system also shown in Figure 4 is related to the $x_1 y_1 z_1$ triad by the transformation matrix

$$\begin{pmatrix} x \\ y \\ z \end{pmatrix} = \begin{pmatrix} \cos\frac{\alpha}{2} & -\sin\frac{\alpha}{2} & 0 \\ \sin\frac{\alpha}{2} & \cos\frac{\alpha}{2} & 0 \\ 0 & 0 & 1 \end{pmatrix} \begin{pmatrix} x_1 \\ y_1 \\ z_1 \end{pmatrix} + \begin{pmatrix} \left(R + \frac{\lambda}{2}\sin\theta\right)\cos\frac{\alpha}{2} \\ \left(R + \frac{\lambda}{2}\sin\theta\right)\sin\frac{\alpha}{2} \\ 0 \end{pmatrix} \tag{4}$$

The xyz nonspinning coordinate system is then related to the axes of symmetry of the paddle arm by substituting Eq. (3) into Eq. (4)
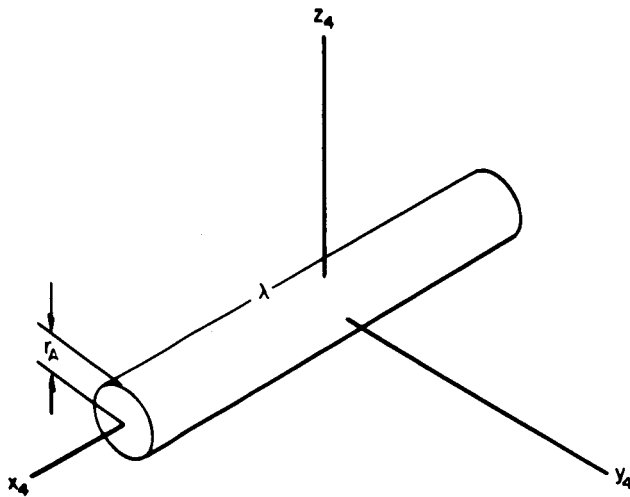
3

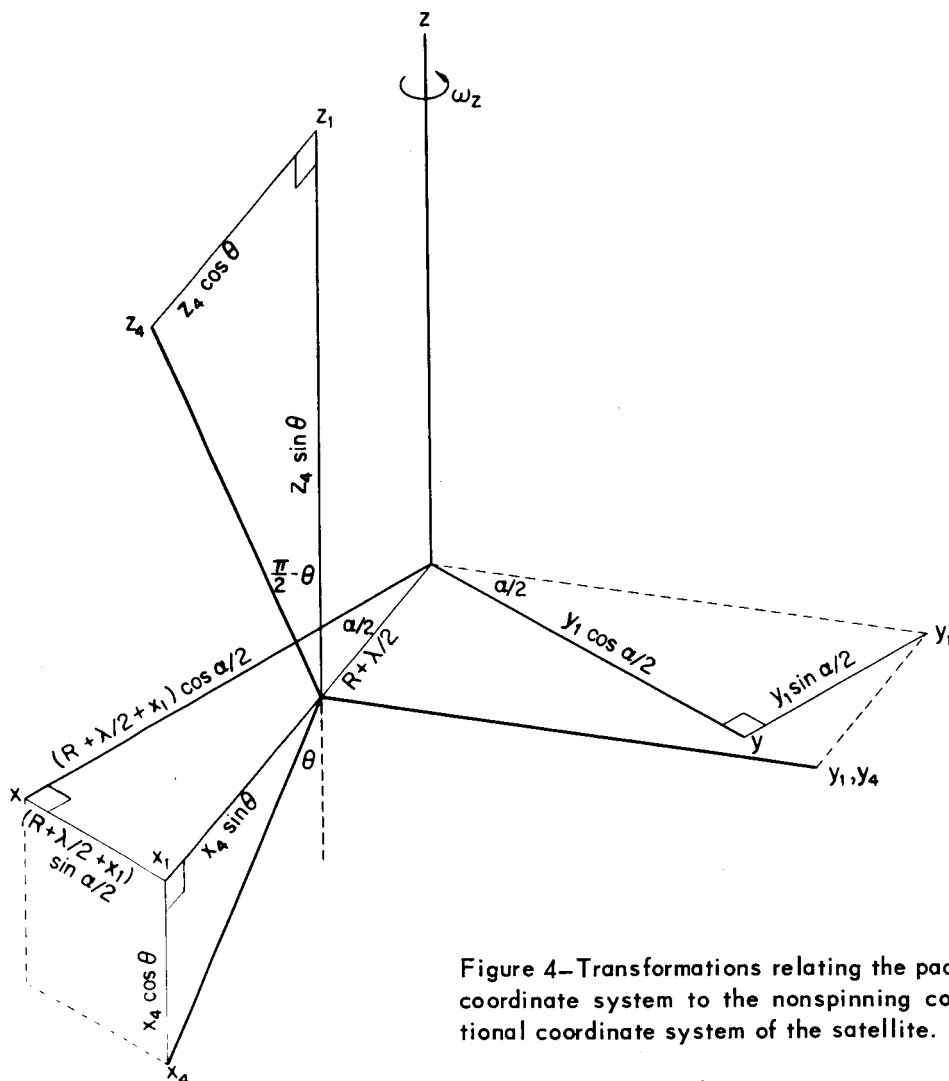Figure 3—Cylindrical paddle arm in its configurational coordinate system.

Figure 4—Transformations relating the paddle-arm coordinate system to the nonspinning configurational coordinate system of the satellite.

4

$$
\begin{pmatrix} x \\ y \\ z \end{pmatrix} = \begin{pmatrix} \cos\dfrac{\alpha}{2}\sin\theta & -\sin\dfrac{\alpha}{2} & \cos\dfrac{\alpha}{2}\cos\theta \\ \sin\dfrac{\alpha}{2}\sin\theta & \cos\dfrac{\alpha}{2} & \sin\dfrac{\alpha}{2}\cos\theta \\ -\cos\theta & 0 & \sin\theta \end{pmatrix} \begin{pmatrix} x_4 \\ y_4 \\ z_4 \end{pmatrix} + \begin{pmatrix} \left(R + \dfrac{\lambda}{2}\sin\theta\right)\cos\dfrac{\alpha}{2} \\ \left(R + \dfrac{\lambda}{2}\sin\theta\right)\sin\dfrac{\alpha}{2} \\ 0 \end{pmatrix} \tag{5}
$$

The moment of inertia of a paddle arm about the satellite spin axis is given by

$$
I_{A_{zz}}(\theta) = \int_m (x^2 + y^2)\,dm = \rho_v \int_v (x^2 + y^2)\,dv \tag{6}
$$

where ρ_v is the uniform mass density of the paddle arm. Substituting the values for x and y from Eq. (5) into Eq. (6) with the appropriate integral limits gives

$$
I_{A_{zz}}(\theta) = \rho_v \int_{-r_A}^{r_A} \int_{-\sqrt{r_A^2 - z_4^2}}^{\sqrt{r_A^2 - z_4^2}} \int_{-\frac{\lambda}{2}}^{\frac{\lambda}{2}} \Bigg[\sin^2\theta\, x_4^2 + y_4^2 + \cos^2\theta\, z_4^2
$$

$$
+ \left(R + \frac{\lambda}{2}\sin\theta\right)^2 + \sin 2\theta\, x_4 z_4 + 2\sin\theta \left(R + \frac{\lambda}{2}\sin\theta\right) x_4
$$

$$
+ 2\cos\theta \left(R + \frac{\lambda}{2}\sin\theta\right) z_4 \Bigg] dx_4\, dy_4\, dz_4 \tag{7}
$$

Integrating Eq. (7) gives

$$
I_{A_{zz}}(\theta) = M_A \left[\frac{\lambda^2}{12}\sin^2\theta + \frac{r_A^2}{4}(1 + \cos^2\theta) + \left(R + \frac{\lambda}{2}\sin\theta\right)^2 \right] \tag{8}
$$

where M_A is the mass of the paddle arm. Since

$$\sin (\pi - \theta) = \sin \theta \qquad (8a)$$

$$\cos^2 (\pi - \theta) = \cos^2 \theta \qquad (8b)$$

then $I_{A_{zz}}(\theta)$ is symmetrical about the paddle-spar angle $\pi/2$ in the range $0 \le \theta \le \pi$.

Rectangular Solar Paddle

One of the rectangular solar paddles is shown in Figure 5. Again mass homogeneity is assumed to exist. The $x_3 y_3 z_3$ triad is the axes of figure symmetry. The length of the paddle is shown as b, the width as a, and the thickness as c. In the case of a symmetrically tapered paddle, c would be approximately the mean thickness.
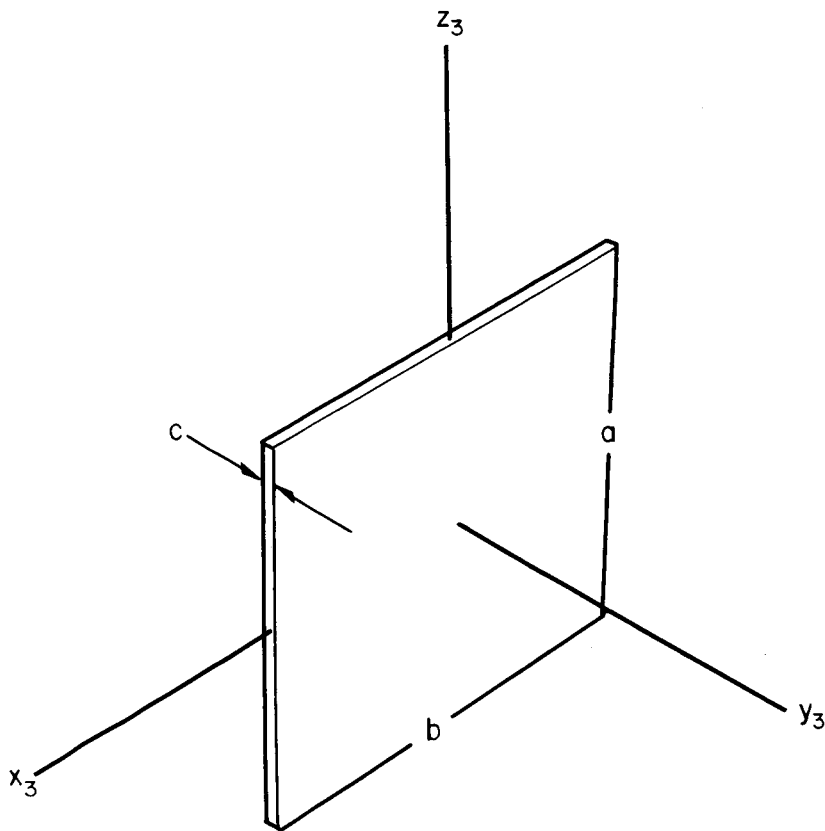

Figure 5—Rectangular solar paddle in its configurational coordinate system.
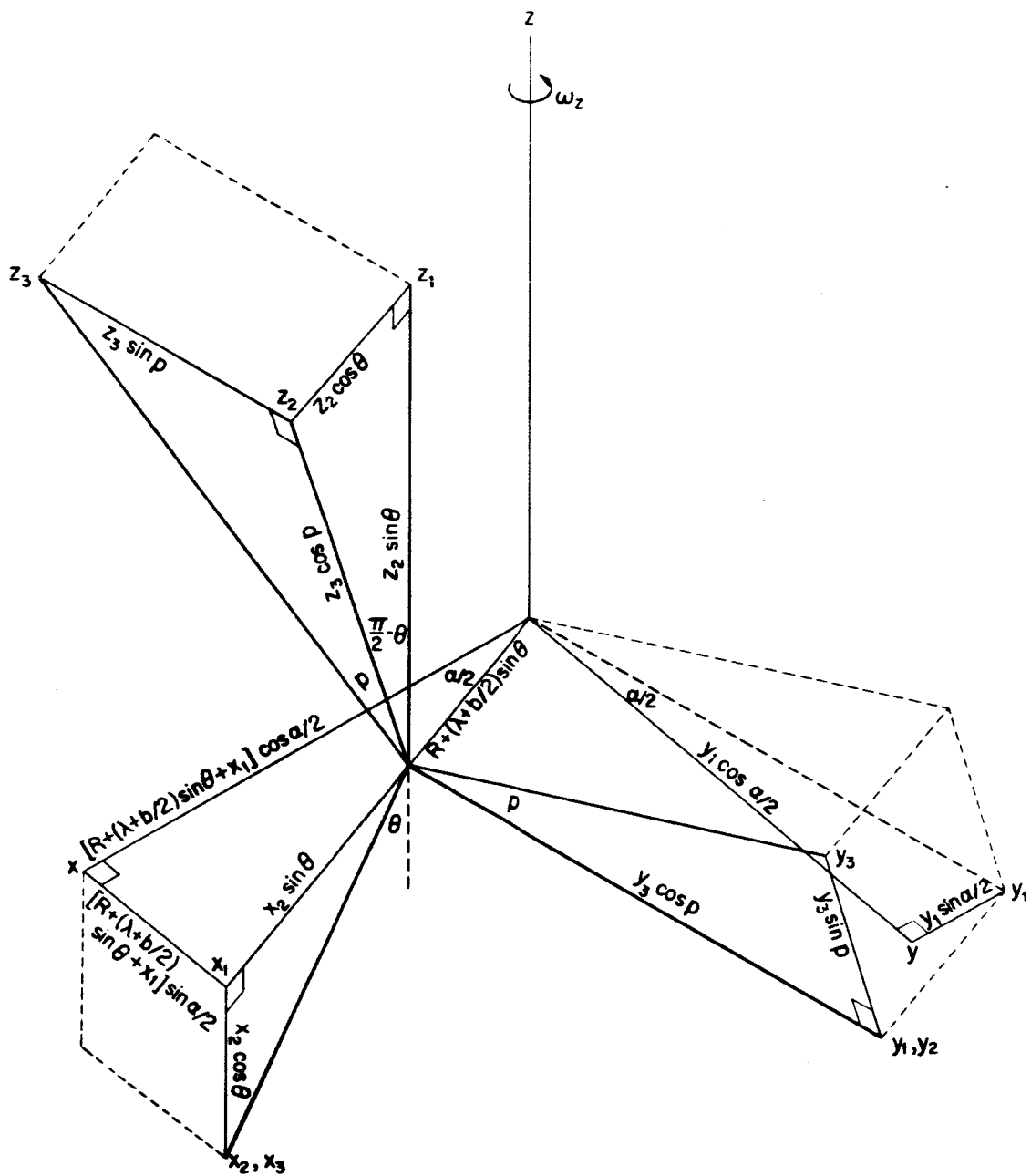
6

Figure 6—Transformations relating the solar-paddle coordinate system to the nonspinning configurational coordinate system of the satellite.

The $x_2 y_2 z_2$ triad is related to the $x_3 y_3 z_3$ axes of symmetry as shown in Figure 6 by the transformation matrix

$$\begin{pmatrix} x_2 \\ y_2 \\ z_2 \end{pmatrix} = \begin{pmatrix} 1 & 0 & 0 \\ 0 & \cos p & -\sin p \\ 0 & \sin p & \cos p \end{pmatrix} \begin{pmatrix} x_3 \\ y_3 \\ z_3 \end{pmatrix} \tag{9}$$

The $x_1 y_1 z_1$ triad is related to the $x_2 y_2 z_2$ triad which is also shown in Figure 6 by the transformation matrix

$$\begin{pmatrix} x_1 \\ y_1 \\ z_1 \end{pmatrix} = \begin{pmatrix} \sin\theta & 0 & \cos\theta \\ 0 & 1 & 0 \\ -\cos\theta & 0 & \sin\theta \end{pmatrix} \begin{pmatrix} x_2 \\ y_2 \\ z_2 \end{pmatrix} \tag{10}$$

The $x_1 y_1 z_1$ triad is then related to the $x_3 y_3 z_3$ axes of paddle symmetry by the substituting Eq. (9) into Eq. (10)

$$\begin{pmatrix} x_1 \\ y_1 \\ z_1 \end{pmatrix} = \begin{pmatrix} \sin\theta & \cos\theta\sin p & \cos\theta\cos p \\ 0 & \cos p & -\sin p \\ -\cos\theta & \sin\theta\sin p & \sin\theta\cos p \end{pmatrix} \begin{pmatrix} x_3 \\ y_3 \\ z_3 \end{pmatrix} \tag{11}$$

The nonspinning coordinate system xyz is related to the $x_1 y_1 z_1$ triad as shown in Figure 6 by the transformation matrix

$$\begin{pmatrix} x \\ y \\ z \end{pmatrix} = \begin{pmatrix} \cos\frac{\alpha}{2} & -\sin\frac{\alpha}{2} & 0 \\ \sin\frac{\alpha}{2} & \cos\frac{\alpha}{2} & 0 \\ 0 & 0 & 1 \end{pmatrix} \begin{pmatrix} x_1 \\ y_1 \\ z_1 \end{pmatrix} + \begin{pmatrix} \left[R + \left(\lambda + \frac{b}{2}\right)\sin\theta \right]\cos\frac{\alpha}{2} \\ \left[R + \left(\lambda + \frac{b}{2}\right)\sin\theta \right]\sin\frac{\alpha}{2} \\ 0 \end{pmatrix} \tag{12}$$

8

The xyz nonspinning coordinate system is then related to the $x_3 y_3 z_3$ axes of paddle symmetry by substituting Eq. (11) into Eq. (12).

$$
\begin{pmatrix} x \\ y \\ z \end{pmatrix} = T \begin{pmatrix} x_3 \\ y_3 \\ z_3 \end{pmatrix} + \begin{pmatrix} \left[R + \left(\lambda + \dfrac{b}{2} \right) \sin \theta \right] \cos \dfrac{\alpha}{2} \\ \left[R + \left(\lambda + \dfrac{b}{2} \right) \sin \theta \right] \sin \dfrac{\alpha}{2} \\ 0 \end{pmatrix} \tag{13}
$$

where

$$
T = \begin{pmatrix}
\cos \dfrac{\alpha}{2} \sin \theta & \cos \dfrac{\alpha}{2} \cos \theta \sin p - \sin \dfrac{\alpha}{2} \cos p & \cos \dfrac{\alpha}{2} \cos \theta \cos p + \sin \dfrac{\alpha}{2} \sin p \\
\sin \dfrac{\alpha}{2} \sin \theta & \sin \dfrac{\alpha}{2} \cos \theta \sin p + \cos \dfrac{\alpha}{2} \cos p & \sin \dfrac{\alpha}{2} \cos \theta \cos p - \cos \dfrac{\alpha}{2} \sin p \\
- \cos \theta & \sin \theta \sin p & \sin \theta \cos p
\end{pmatrix} \tag{14}
$$

The moment of inertia of the rectangular paddle about the satellite spin axis is given by

$$
I_{P_{zz}} (p, \theta) = \int_m (x^2 + y^2) \, dm = \rho_v \int_{-a/2}^{a/2} \int_{-c/2}^{c/2} \int_{-b/2}^{b/2} (x^2 + y^2) \, dx_3 \, dy_3 \, dz_3 \tag{15}
$$

9

where ρ_v is the uniform mass density of the rectangular paddle. Substituting the values for x and y from Eq. (13) into Eq. (15) and then integrating gives

$$I_{P_{zz}}(p, \theta) = M_P \left\{ \frac{a^2}{12} (\cos^2 \theta \cos^2 p + \sin^2 p) + \frac{b^2}{12} \sin^2 \theta + \frac{c^2}{12} (\cos^2 \theta \sin^2 p + \cos^2 p) \right.$$

$$\left. + \left[R + \left(\lambda + \frac{b}{2} \right) \sin \theta \right]^2 \right\} \tag{16}$$

where M_P is the mass of the paddle. Since

$$\sin (\pi - \theta) = \sin \theta \tag{16a}$$

$$\cos^2 (\pi - \theta) = \cos^2 \theta \tag{16b}$$

then $I_{P_{zz}}(p, \theta)$ is symmetrical about the paddle-spar angle $\pi/2$ in the range $0 \leq \theta \leq \pi$. Similarly it is noted that $I_{P_{zz}}(p, \theta)$ is symmetrical in the range $0 \leq p \leq \pi$ about the paddle-pitch angle $\pi/2$, and is symmetrical in the range $-\pi/2 \leq p \leq \pi/2$ about the paddle-pitch angle zero.

SATELLITE SPIN RATE ANALYSIS

The conservation of angular momentum states that for a constant paddle-pitch angle and no external torques

$$H_0(\theta) = H(\theta) \tag{17}$$

where $H_0(\theta)$ is the initial satellite angular momentum at a constant paddle-pitch angle and a paddle-spar angle equal to zero, and $H(\theta)$ is the satellite angular momentum as a function of paddle-spar angle only. Hence, Eq. (17) can be expressed as

$$\left[I_{B_{zz}} + 4 \left(I_{A_{zz}}(0) + I_{P_{zz}}(p, 0) \right) \right]_p \omega_{z_{\theta_0}} = \left[I_{B_{zz}} + 4 \left(I_{A_{zz}}(\theta) + I_{P_{zz}}(p, \theta) \right) \right]_p \omega_{z_\theta} \tag{18}$$

where identical paddles and paddle arms are assumed.

The satellite normalized-spin rate due to a change in paddle-spar angle becomes

$$\frac{\omega_{z_\theta}}{\omega_{z_{\theta_0}}} = \frac{\left[I_{B_{zz}} + 4\left(I_{A_{zz}}(0) + I_{P_{zz}}(p,\ 0)\right)\right]_p}{\left[I_{B_{zz}} + 4\left(I_{A_{zz}}(\theta) + I_{P_{zz}}(p,\ \theta)\right)\right]_p} \qquad (19)$$

This equation is used in the appendices to calculate the satellite normalized-spin rate as a function of paddle-spar angle from 0 to π for the laboratory model satellite and the IMP-type satellite.

Similarly for a paddle-pitch-angle change, the conservation law states that for no external torques

$$H_0(p) = H(p) \qquad (20)$$

where $H_0(p)$ is the initial satellite angular momentum at a constant paddle-spar angle and a paddle-pitch angle equal to zero, and $H(p)$ is the satellite angular momentum as a function of paddle-pitch angle only. Hence, Eq. (20) can be expressed as

$$\left[I_{B_{zz}} + 4\left(I_{A_{zz}}(\theta) + I_{P_{zz}}(0,\ \theta)\right)\right]_\theta \omega_{z_{P_0}} = \left[I_{B_{zz}} + 4\left(I_{A_{zz}}(\theta) + I_{P_{zz}}(p,\ \theta)\right)\right]_\theta \omega_{z_p} \qquad (21)$$

where again identical paddles and paddle arms are assumed.

The satellite normalized-spin rate due to a change in paddle-pitch angle is then given by

$$\frac{\omega_{z_P}}{\omega_{z_{P_0}}} = \frac{\left[I_{B_{zz}} + 4\left(I_{A_{zz}}(\theta) + I_{P_{zz}}(0,\ \theta)\right)\right]_\theta}{\left[I_{B_{zz}} + 4\left(I_{A_{zz}}(\theta) + I_{P_{zz}}(p,\ \theta)\right)\right]_\theta} \qquad (22)$$

This equation is used in the appendices to calculate the satellite spin decay due to change in paddle-pitch angle from 0 to $\pi/2$ for both satellites.

11

DISCUSSION

The moment of inertia of a solar paddle at constant paddle-pitch angle and a paddle-spar angle equal to zero is given by Eq. (16)

$$I_{P_{zz}}(p,0) = M_P \left(\frac{a^2}{12} + \frac{c^2}{12} + R^2 \right) \qquad (23)$$

Similarly for a paddle-spar angle equal to $\pi/2$

$$I_{P_{zz}}(p,\pi/2) = M_P \left\{ \frac{a^2}{12} \sin^2 p + \frac{b^2}{12} + \frac{c^2}{12} \cos^2 p + \left[R + \left(\lambda + \frac{b}{2} \right) \right]^2 \right\} \qquad (24)$$

Hence

$$I_{P_{zz}}(p,\pi/2) - I_{P_{zz}}(p,0) = M_P \left\{ \frac{1}{12}(b^2 - c^2 \sin^2 p) + \left(\lambda + \frac{b}{2} \right) \left[\left(\lambda + \frac{b}{2} \right) + 2R \right] - \frac{a^2}{12} \cos^2 p \right\}$$

Now if $\qquad (25)$

$$\frac{c^2}{12} \sin^2 p + \frac{a^2}{12} \cos^2 p \le \frac{c^2 + a^2}{12} < \frac{b^2}{12} + \left(\lambda + \frac{b}{2} \right) \left[\left(\lambda + \frac{b}{2} \right) + 2R \right] \qquad (26)$$

which is satisfied by both satellites discussed in the appendices, then the previous expression becomes the inequality

$$I_{P_{zz}}(p,0) < I_{P_{zz}}(p,\pi/2) \qquad (27)$$

The moment of inertia of a paddle arm for a paddle-spar angle equal to zero is given by Eq. (8)

$$I_{A_{zz}}(0) = M_A \left(\frac{r_A^2}{2} + R^2 \right) \qquad (28)$$

Similarly for a paddle-spar angle equal to $\pi/2$

$$I_{A_{zz}}(\pi/2) = M_A \left[\frac{\lambda^2}{12} + \frac{r_A^2}{4} + \left(R + \frac{\lambda}{2} \right)^2 \right] \qquad (29)$$

12

Hence

$$I_{A_{zz}}\left(\frac{\pi}{2}\right) - I_{A_{zz}}(0) = M_A \left[\left(\frac{\lambda^2}{3} + R\lambda\right) - \frac{r_A^2}{4} \right] \tag{30}$$

Now if

$$\frac{r_A^2}{4} < \frac{\lambda^2}{3} + R\lambda \tag{31}$$

which is satisfied by both satellites discussed in the appendices, then the previous expression becomes the inequality

$$I_{A_{zz}}(0) < I_{A_{zz}}\left(\frac{\pi}{2}\right) \tag{32}$$

The addition of $I_{B_{zz}}$ to four times the sum of Ineqs. (27) and (32) gives

$$\left[I_{B_{zz}} + 4\left(I_{A_{zz}}(0) + I_{P_{zz}}(p, 0)\right) \right]_p < \left[I_{B_{zz}} + 4\left(I_{A_{zz}}\left(\frac{\pi}{2}\right) + I_{P_{zz}}\left(p, \frac{\pi}{2}\right)\right) \right]_p \tag{33}$$

or

$$\frac{\omega_{z_{\theta=\frac{\pi}{2}}}}{\omega_{z_{\theta_0}}} = \frac{\left[I_{B_{zz}} + 4\left(I_{A_{zz}}(0) + I_{P_{zz}}(p, 0)\right) \right]_p}{\left[I_{B_{zz}} + 4\left(I_{A_{zz}}\left(\frac{\pi}{2}\right) + I_{P_{zz}}\left(p, \frac{\pi}{2}\right)\right) \right]_p} < 1 \tag{34}$$

Hence, from the above expression, the satellite spin rate due to a paddle-spar angle increase in the range $0 \leq \theta \leq \pi/2$ would gradually decay for both satellites. Conversely, the satellite spin rate due to a paddle-spar angle decrease in the same range would gradually grow for both satellites.

The moment of inertia of a solar paddle with constant paddle-spar angle and a paddle-pitch angle equal to zero is given by Eq. (16)

$$I_{P_{zz}}(0, \theta) = M_P \left\{ \frac{a^2}{12} \cos^2\theta + \frac{b^2}{12} \sin^2\theta + \frac{c^2}{12} + \left[R + \left(\lambda + \frac{b}{2}\right)\sin\theta \right]^2 \right\} \tag{35}$$

13

Similarly for a paddle-pitch angle equal to $\pi/2$

$$I_{P_{zz}}\left(\frac{\pi}{2},\,\theta\right) = M_P\left\{\frac{a^2}{12} + \frac{b^2}{12}\sin^2\theta + \frac{c^2}{12}\cos^2\theta + \left[R + \left(\lambda + \frac{b}{2}\right)\sin\theta\right]^2\right\} \quad (36)$$

Hence

$$I_{P_{zz}}\left(\frac{\pi}{2},\,\theta\right) - I_{P_{zz}}(0,\,\theta) = M_P\left(\frac{a^2 - c^2}{12}\right)\sin^2\theta \quad (37)$$

Now if

$$c < a \quad (38)$$

which is satisfied by both satellites discussed in the appendices, then the previous expression becomes

$$I_{P_{zz}}(0,\,\theta) < I_{P_{zz}}\left(\frac{\pi}{2},\,\theta\right) \quad (39)$$

The addition of $I_{B_{zz}}$ and $4\,I_{A_{zz}}(\theta)$ to four times the Ineq. (39) gives

$$\left[I_{B_{zz}} + 4\left(I_{A_{zz}}(\theta) + I_{P_{zz}}(0,\,\theta)\right)\right]_\theta < \left[I_{B_{zz}} + 4\left(I_{A_{zz}}(\theta) + I_{P_{zz}}\left(\frac{\pi}{2},\,\theta\right)\right)\right]_\theta \quad (40)$$

or

$$\frac{\omega_{z_{P=\frac{\pi}{2}}}}{\omega_{z_{P0}}} = \frac{\left[I_{B_{zz}} + 4\left(I_{A_{zz}}(\theta) + I_{P_{zz}}(0,\,\theta)\right)\right]_\theta}{\left[I_{B_{zz}} + 4\left(I_{A_{zz}}(\theta) + I_{P_{zz}}\left(\frac{\pi}{2},\,\theta\right)\right)\right]_\theta} < 1 \quad (41)$$

Hence from Eq. (41), the satellite spin rate due to a paddle-pitch angle increase in the range $0 \le p \le \pi/2$ would gradually decay for both satellites. Conversely, the satellite spin rate due to a paddle-pitch angle decrease in the same range would tend to grow for both satellites. From Eqs. (8) and (16) it can be seen that Eqs. (19) and (22) are symmetrical about the paddle-spar angle $\pi/2$ and the paddle-pitch angle $\pi/2$, respectively.

In the appendices, curves made from specific calculations based on the geometry of the two satellites bear out the conclusions of this discussion.

14

APPENDIX A

Calculations, Results, and Curves Concerning
the Laboratory Model Satellite

The values of the parameters involved in calculating the expressions for the various moment of inertia components and satellite normalized spin rates for the laboratory model satellite are

a = 5.00 in.

b = 6.50 in.

c = 3.75×10^{-1} in.

h = 2.13 in.

M_A = 3.34×10^{-4} slugs

M_B = 3.13×10^{-1} slugs

M_P = 6.89×10^{-3} slugs

R = 3.75 in.

r = 3.46 in.

r_A = 1.25×10^{-1} in.

s = 2.87 in.

λ = 2.25 in.

The value of the moment of inertia for the satellite body about its spin axis, using Eq. (2) becomes

$$I_{B_{zz}} = \left(\frac{3.13 \times 10^{-1}}{24} \right) \left[(2.87)^2 + 12\,(3.46)^2 \right] = 1.98 \text{ slug-in}^2 \quad \text{(A-1)}$$

The value of the moment of inertia for a paddle arm about the z-axis of the nonspinning configurational coordinate system, using Eq. (8) becomes

$$I_{A_{zz}}(\text{slug-in}^2) = (5.64 \times 10^{-4}) \sin^2 \theta + (1.31 \times 10^{-6}) \cos^2 \theta$$

$$+ (2.82 \times 10^{-3}) \sin \theta + 4.70 \times 10^{-3} \quad \text{(A-2)}$$

This expression is plotted in Figure A-1 as a function of the paddle-spar angle θ.
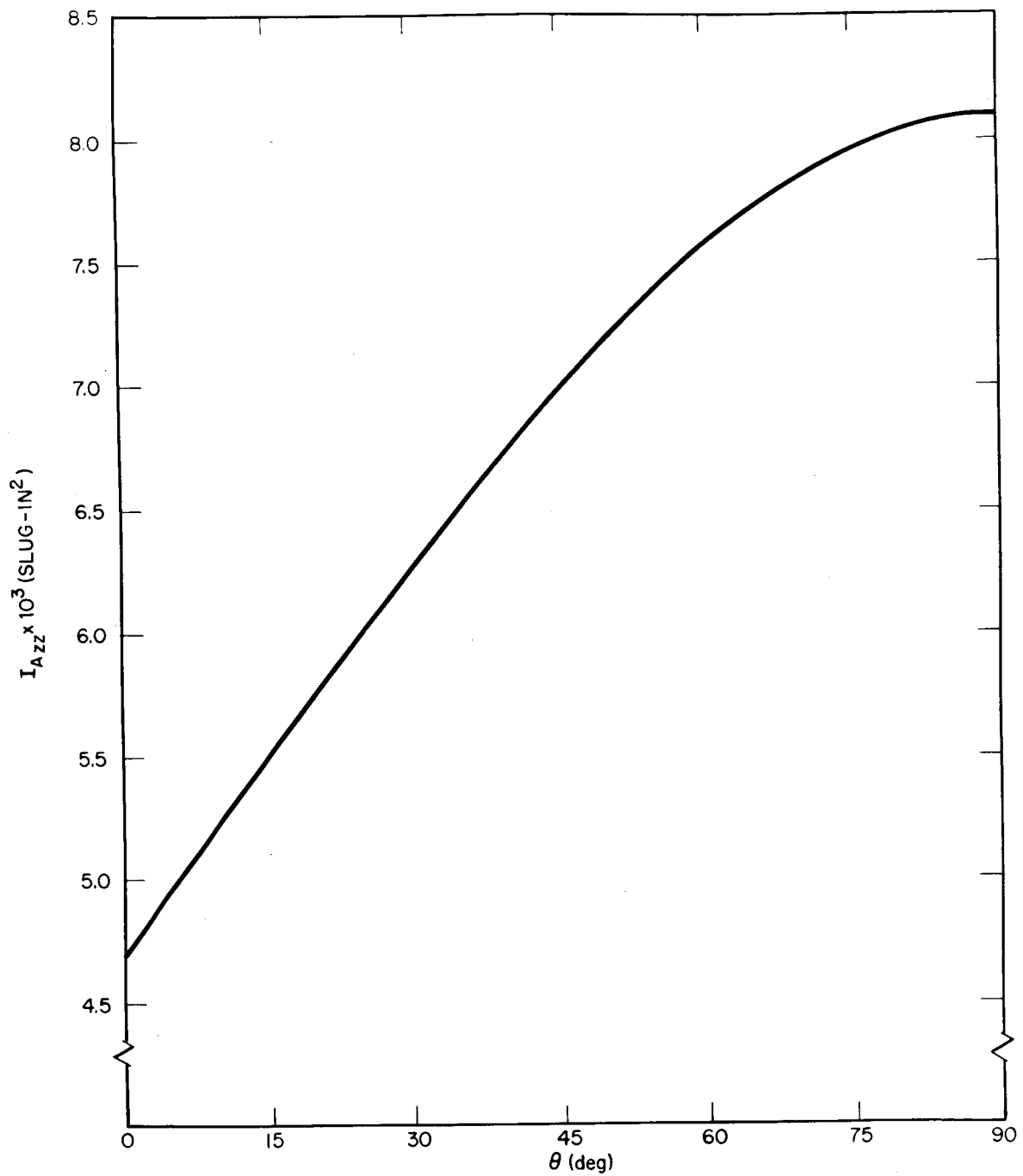
15

Figure A-1—Moment of inertia about the satellite spin axis of the model paddle
arm as a function of paddle-spar angle.

16

The value of the moment of inertia for a solar paddle about the z-axis of the nonspinning configurational coordinate system, using Eq. (16) becomes

$$I_{P_{zz}}(\text{slug-in}^2) = (2.33 \times 10^{-1}) \sin^2 \theta + [(8.07 \times 10^{-5}) \sin^2 p$$

$$+ (1.43 \times 10^{-2}) \cos^2 p] \cos^2 \theta + (2.84 \times 10^{-1}) \sin \theta$$

$$+ (1.43 \times 10^{-2}) \sin^2 p + (8.07 \times 10^{-5}) \cos^2 p + 9.69 \times 10^{-2}$$

(A-3)

The above expression is plotted in Figure A-2 as a function of the paddle-spar angle θ with the paddle-pitch angle p as the parameter.

The satellite normalized spin rate as a function of paddle-spar angle θ using Eq. (19) becomes

$$\frac{\omega_{z\theta}}{\omega_{z\theta_0}} = \frac{2.44}{1.98 + 4 \left(I_{A_{zz}}(\theta) + I_{P_{zz}}(p, \theta)\right)_p}$$

(A-4)

This expression is plotted in Figure A-3 as a function of the paddle-spar angle θ with the paddle-pitch angle p the parameter.

Similarly the satellite normalized-spin rate as a function of the paddle-pitch angle p using Eq. (22), becomes

$$\frac{\omega_{zp}}{\omega_0} = \frac{(9.34 \times 10^{-1}) \sin^2 \theta + (5.72 \times 10^{-2}) \cos^2 \theta + 1.15 \sin \theta + 2.39}{1.98 + 4 \left(I_{A_{zz}}(\theta) + I_{P_{zz}}(p, \theta)\right)_\theta}$$

(A-5)

The above expression is plotted in Figure A-4 as a function of the paddle-pitch angle p with the paddle-spar angle θ as the parameter.

Results

The curves for satellite spin rate show a decay over the range $0 \leq p$, $\theta \leq \pi/2$ for an increase in either of the orientation angles. The change in spin rate due to a change in paddle-pitch angle p, at constant paddle-spar angle θ, appears to be negligible over the entire range $0 \leq p \leq \pi/2$ — less than 1.5% at any paddle-spar angle.
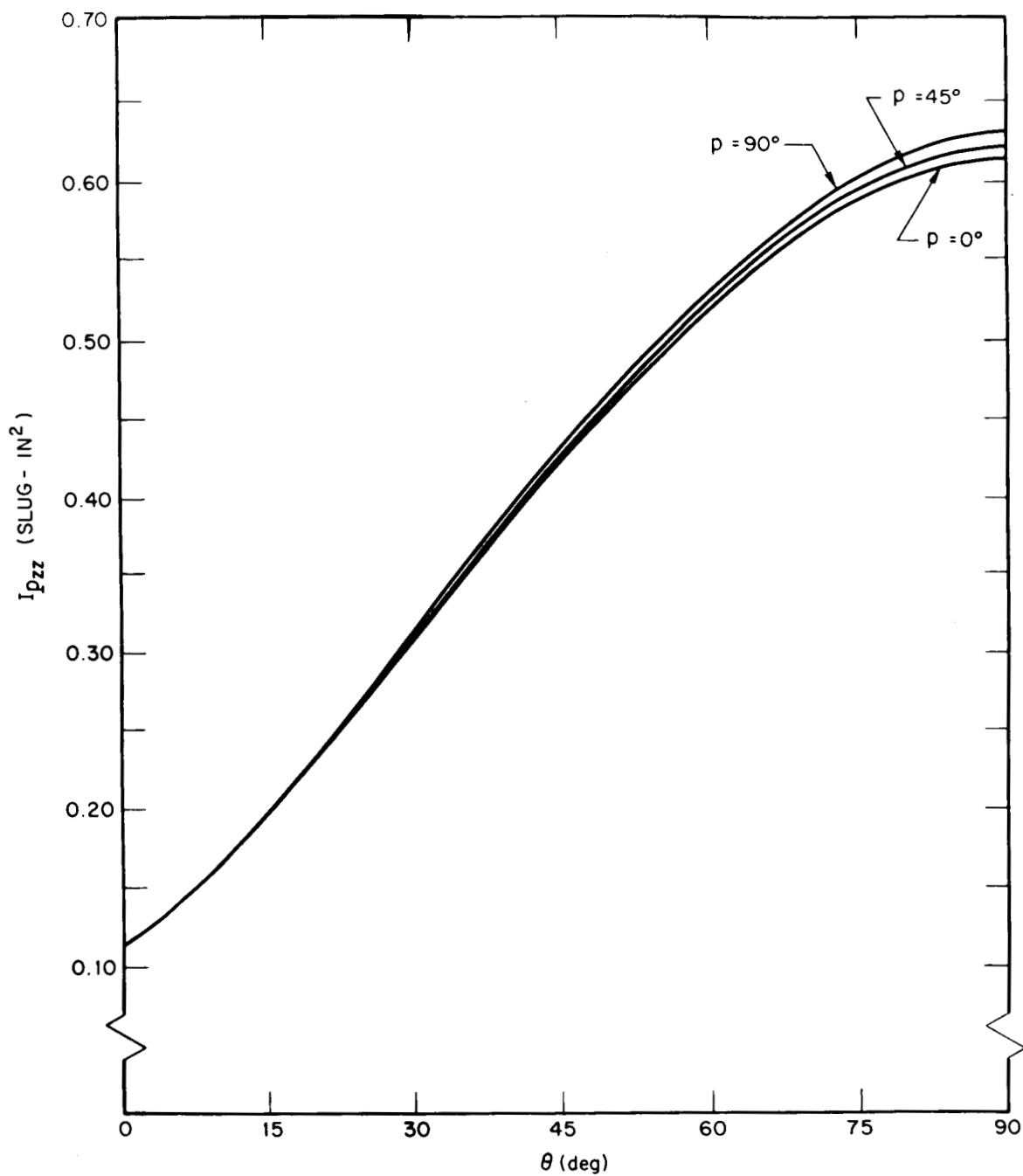
17

Figure A-2—Moment of inertia about the satellite spin axis of the model solar paddle as a function of paddle-spar angle, showing the effect of paddle-pitch angle.
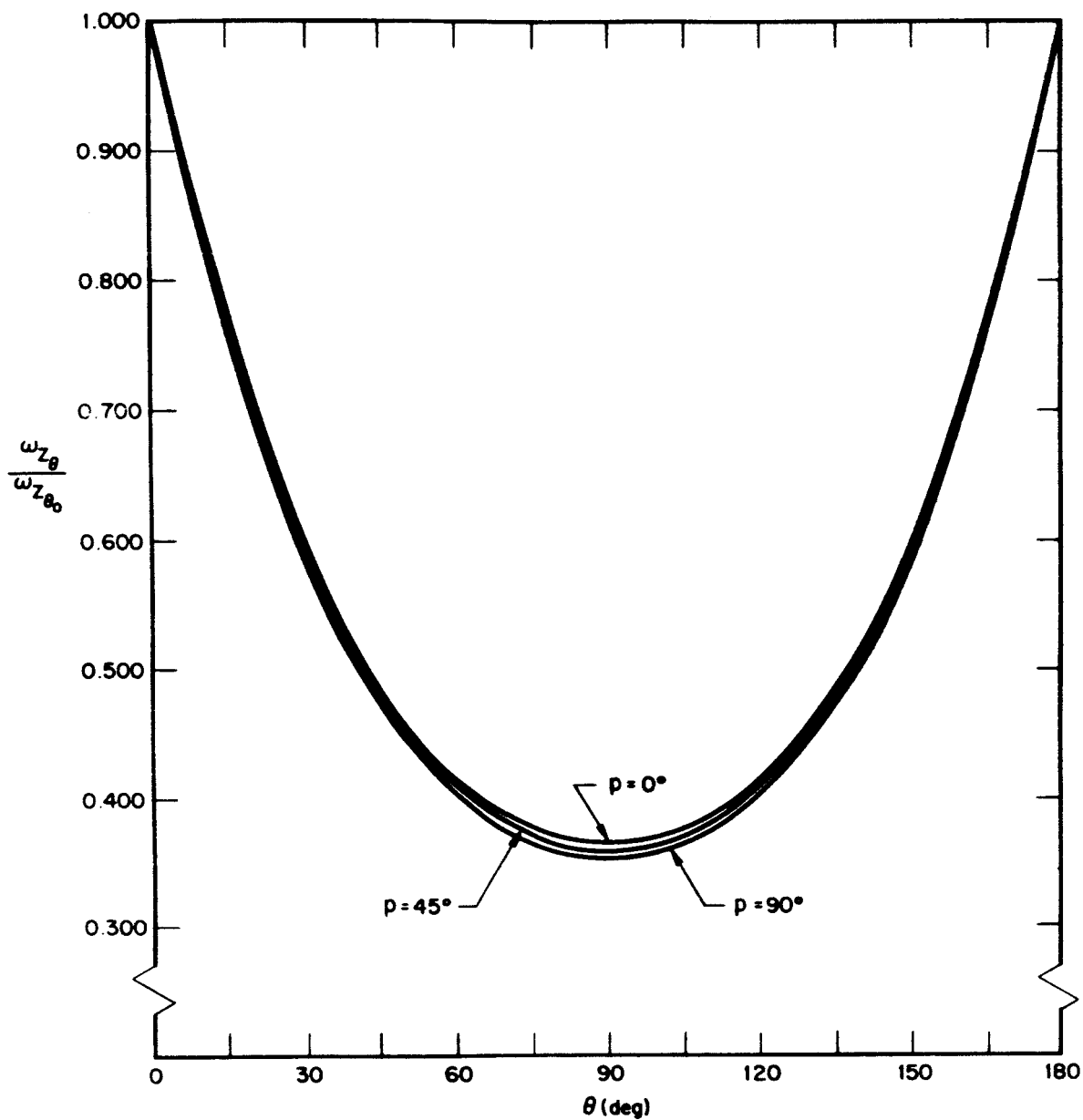
18

Figure A-3—Normalized spin rate of the model satellite as a function of paddle-spar angle, showing the effect of paddle-pitch angle.
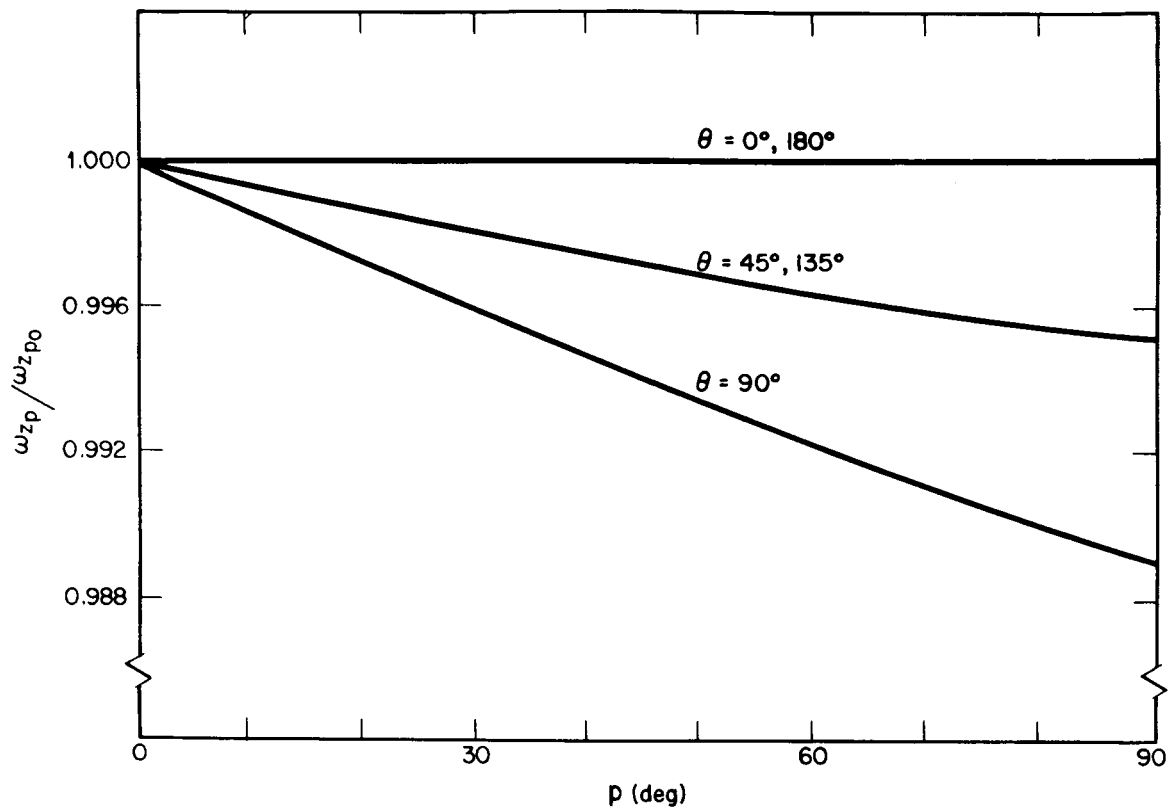
Figure A-4—Normalized spin-rate of the model satellite as a function of paddle-pitch angle, showing the effect of paddle-spar angle.

APPENDIX B

Calculations, Results, and Curves Concerning
an IMP-Type Satellite

The values of the parameters involved in calculating the expressions for the various moment of inertia components and the satellite normalized-spin rates for the IMP-type satellite are

a	= 1.68 ft.	M_P	= 2.06×10^{-1} slugs
b	= 2.17 ft.	R	= 1.22 ft.
c	= 4.17×10^{-2} ft.	r	= 1.12 ft.
h	= 7.08×10^{-1} ft.	r_A	= 3.68×10^{-2} ft.
M_A	= 1.66×10^{-2} slugs	s	= 9.31×10^{-1} ft.
M_B	= 3.44 slugs	λ	= 7.50×10^{-1} ft.

The value of the moment of inertia for the satellite body about its spin axis using Eq. (2), becomes

$$I_{B_{zz}} = \frac{3.44}{24} \left[(9.31 \times 10^{-1})^2 + 12 (1.12)^2 \right] = 2.28 \text{ slug-ft}^2 \qquad (B-1)$$

The value of the moment of inertia for a paddle arm about the z-axis of the non-spinning configurational coordinate system using Eq. (8), becomes

$$I_{A_{zz}}(\text{slug-ft}^2) = (3.11 \times 10^{-3}) \sin^2 \theta + (5.62 \times 10^{-6}) \cos^2 \theta$$

$$+ (1.52 \times 10^{-2}) \sin \theta + 2.47 \times 10^{-2} \qquad (B-2)$$

This expression is plotted in Figure B-1 as a function of the paddle-spar angle θ.

The value of the moment of inertia for a solar paddle about the z-axis of the nonspinning configurational coordinate system using Eq. (16), becomes
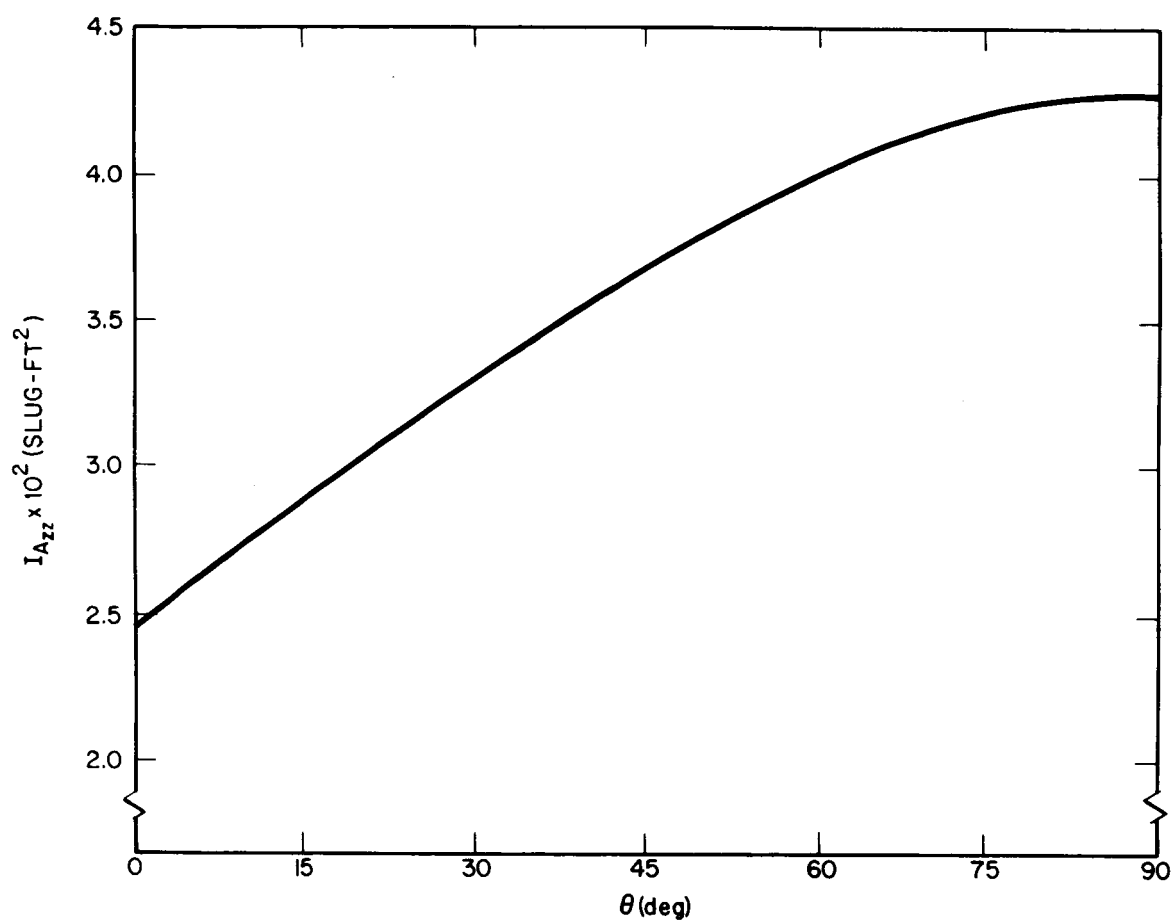
Figure B-1—Moment of inertia about the satellite spin axis of an IMP-type paddle arm, assuming cylindrical symmetry and homogeneity, as a function of paddle-spar angle.

22

$$I_{P_{zz}}(\text{slug-ft}^2) = (7.74 \times 10^{-1}) \sin^2 \theta + [(2.98 \times 10^{-5}) \sin^2 p$$

$$+ (4.84 \times 10^{-2}) \cos^2 p] \cos^2 \theta + (9.22 \times 10^{-1}) \sin \theta$$

$$+ (4.84 \times 10^{-2}) \sin^2 p + (2.98 \times 10^{-5}) \cos^2 p$$

$$+ 3.07 \times 10^{-1} \tag{B-3}$$

The above expression is plotted in Figure B-2 as a function of the paddle-spar angle θ with the paddle-pitch angle p as the parameter.

The satellite normalized-spin rate as a function of paddle-spar angle θ using Eq. (19), becomes

$$\frac{\omega_{z_\theta}}{\omega_{z_{\theta_0}}} = \frac{3.80}{2.28 + 4 \left(I_{A_{zz}}(\theta) + I_{P_{zz}}(p, \theta)\right)_p} \tag{B-4}$$

This expression is plotted in Figure B-3 as a function of the paddle-spar angle θ with the paddle-pitch angle p as the parameter.

Similarly, the satellite normalized-spin rate as a function of the paddle-pitch angle p using Eq. (22), becomes

$$\frac{\omega_{z_p}}{\omega_{z_{p_0}}} = \frac{3.11 \sin^2 \theta + 0.194 \cos^2 \theta + 3.75 \sin \theta + 3.61}{2.28 + 4 \left(I_{A_{zz}}(\theta) + I_{P_{zz}}(p, \theta)\right)_\theta} \tag{B-5}$$

The above expression is plotted in Figure B-4 as a function of the paddle-pitch angle p with the paddle-spar angle θ as the parameter.

Results

Again the curves for satellite spin rate show a decay over the range $0 \leq p$, $\theta \leq \pi/2$ for an increase in either of the orientation angles. The change in spin rate due to a change in paddle-pitch angle p, at constant paddle-spar angle θ, still appears to be negligible over the entire range $0 \leq p \leq \pi/2$ — less than 2.5% at any paddle-spar angle.
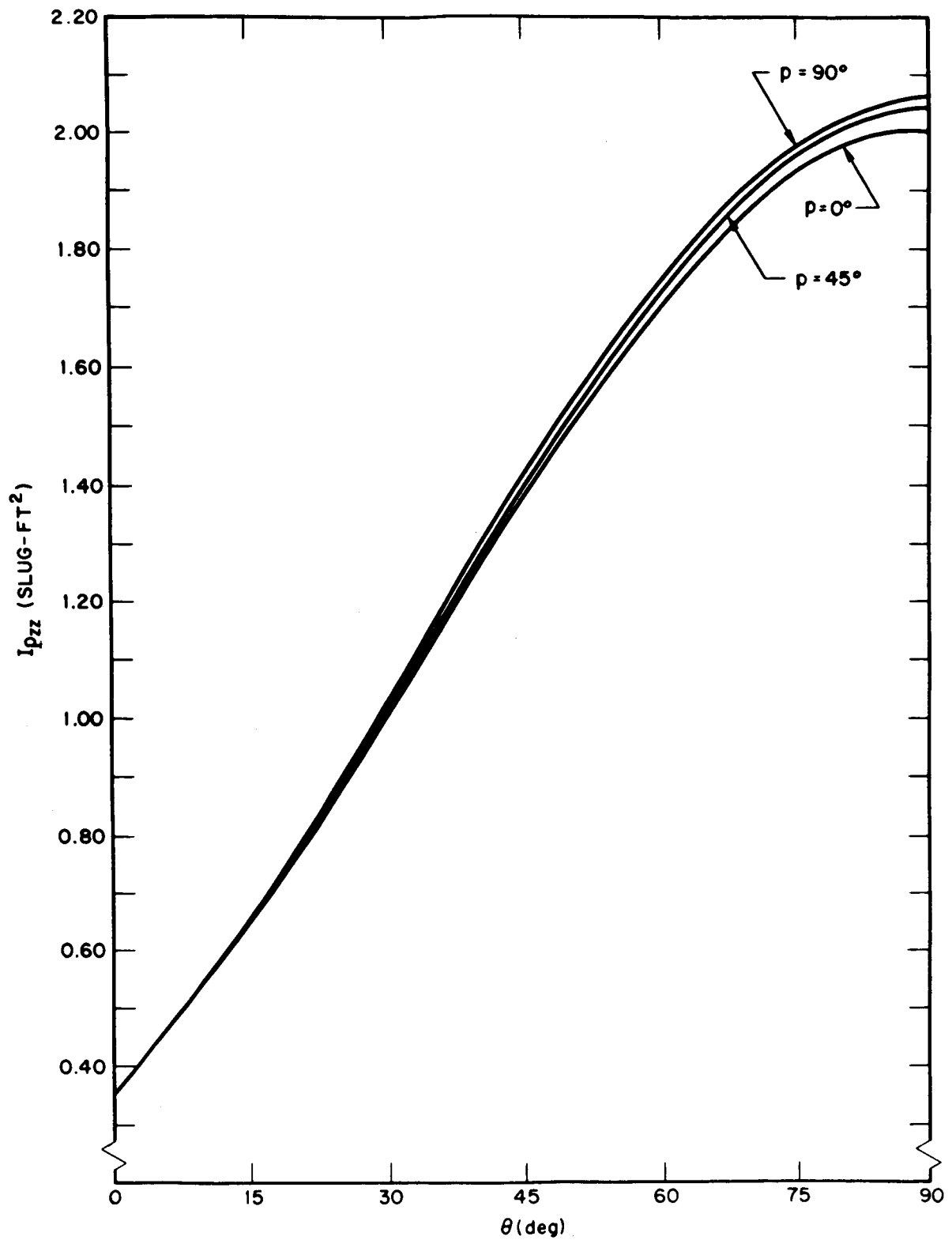
23

Figure B-2—Moment of inertia about the satellite spin axis of an IMP-type solar paddle, assuming rectangularity and homogeneity, as a function of paddle-spar angle, showing the effect of paddle-pitch angle.
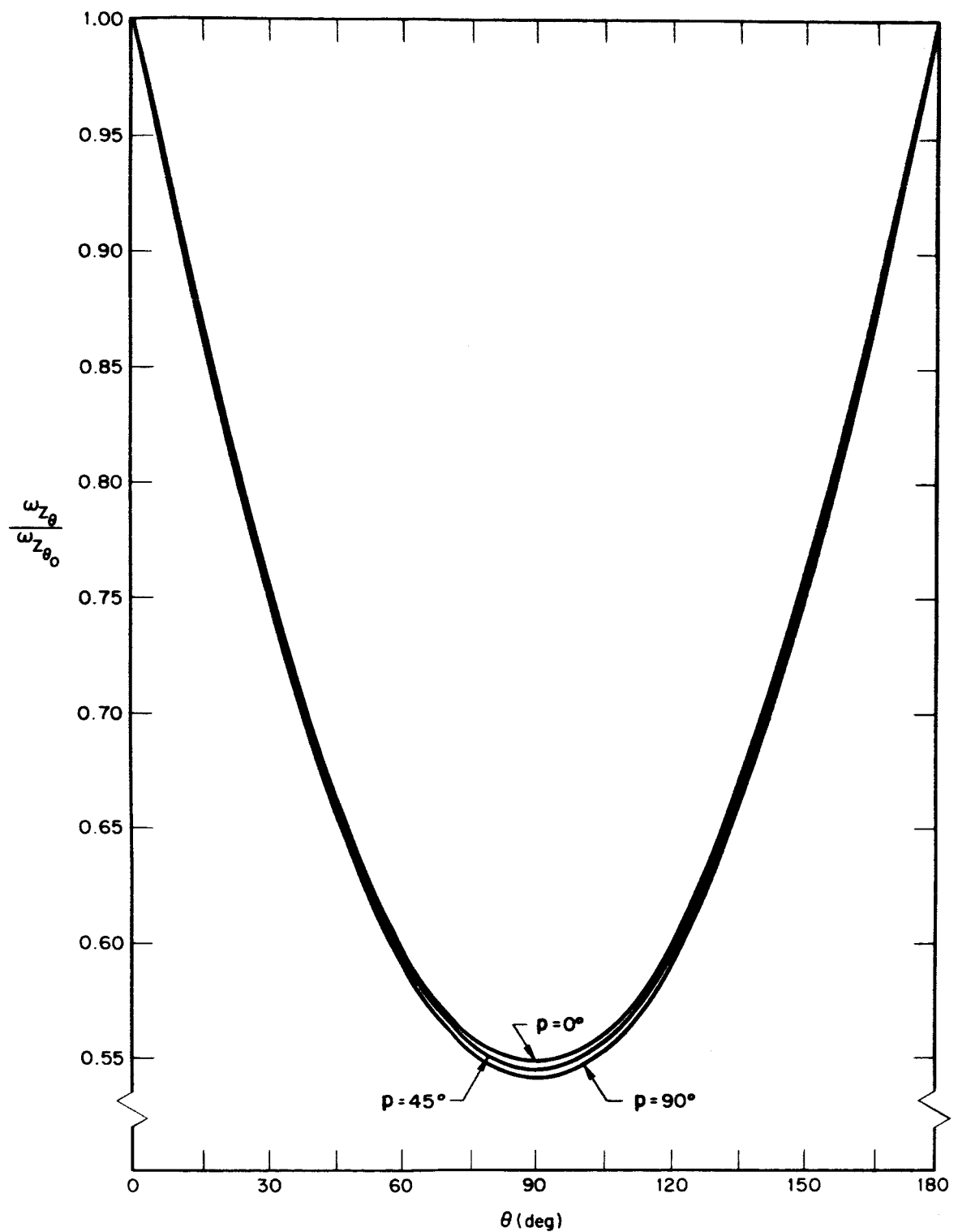
Figure B-3—Normalized spin rate of an IMP-type satellite as a function of paddle-spar angle, showing the effect of paddle-pitch angle.
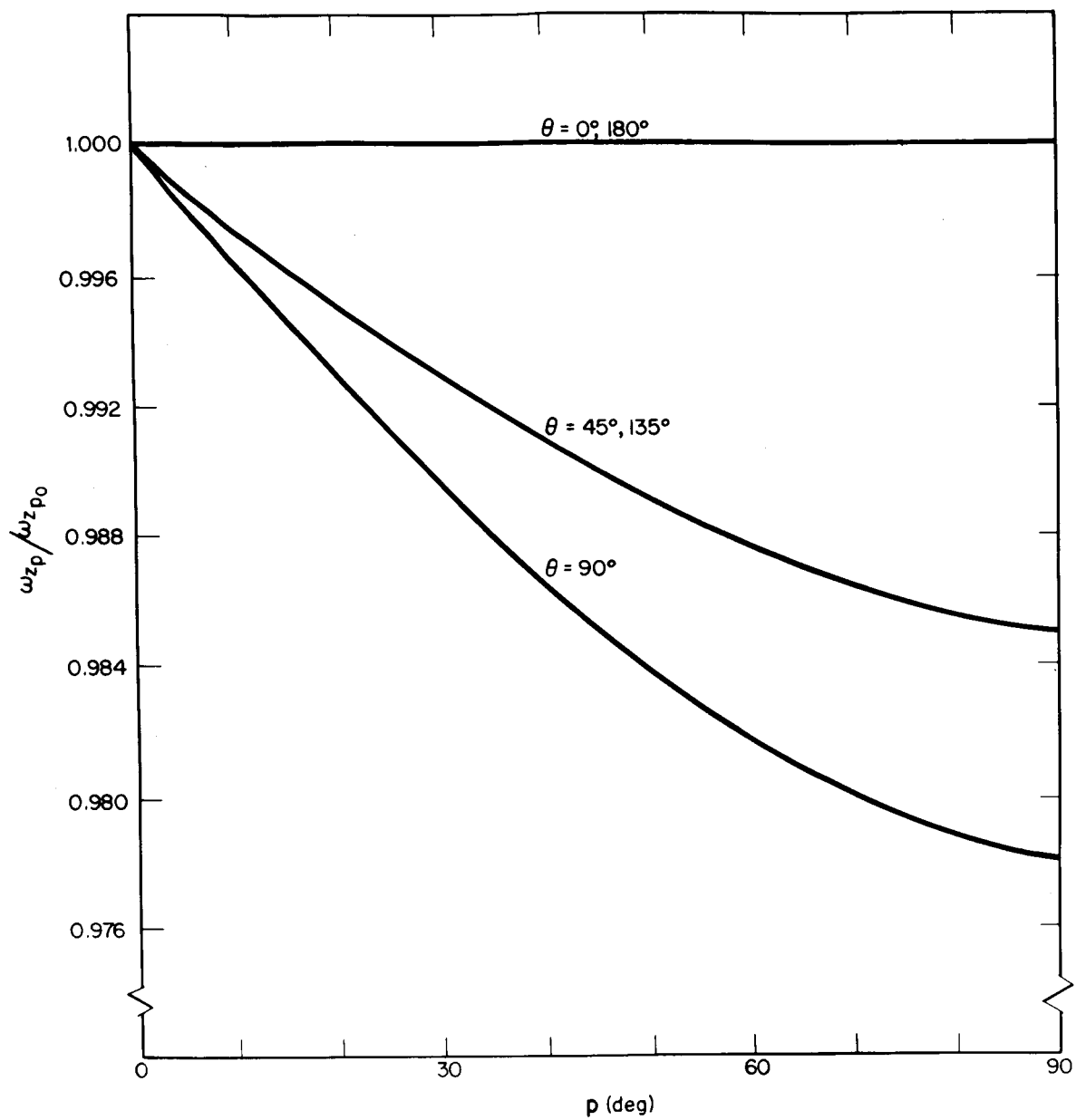
Figure B-4–Normalized spin rate of an IMP-type satellite as a function of paddle-pitch angle, showing the effect of paddle-spar angle.